Ly. J. Appl. Sci. Tech. V. 14, No (1). 51-66
Libya Journal of Applied Sciences and Technology
https://ljast.ly/

Hydro-Power Energy Recovery in Water Pipelines Networks: A Case Study of Man-Made River in Libya

Ahmed Amer Sahab[*1], Munir Eraghubi [2], and Osama Hassin [1]

[1]Department of Mechanical Engineering and Energies, School of Engineering and Applied, Science, Libyan Academy, Tripoli, Libya.
[2] Department of Mechanical Engineering, College of Technical Engineering – Janzour, Tripoli, Libya.

* Ahmed Amer Sahab ahmedsahab88@gmail.com

Article Info

Received: 02/06/2026
Accepted: 27/06/2026
Online publish: 30/06/2026

Keywords:
Hydraulic energy;
Energy recovery;
Man-Made River;

Abstract

The Man-Made River (MMR) in Libya is one of the world's largest water transfer systems, yet it consumes vast amounts of electricity to deliver water across long distances. This research addresses the challenge of energy demand by exploring the recovery of hydraulic energy that is normally wasted as pressure losses within the MMR pipelines. A hydraulic model of the pipeline was developed using EPANET, with actual design data serving as input. Four operational scenarios were evaluated (1.2, 1.3, 2.0, and 2.5 MCMD), and the results were analyzed to estimate recoverable energy and identify suitable turbine types. The methodology included simulation of head and pressure distributions, energy recovery calculations, and comparison with the system's electricity consumption. The study found that at current operating flows (1.2–1.3 MCMD), turbines could recover between 686 and 733 MWh/day, meeting nearly half of the system's electricity demand. At the original design capacity of 2.0 MCMD, recovery declined to about 610 MWh/day, while at 2.5 MCMD the net gain dropped to only 117 MWh/day due to pumping requirements. Francis turbines were identified as the most practical technology, with Pelton turbines as secondary options in high-head conditions. The research demonstrates that hydropower recovery from the MMR is technically feasible and environmentally beneficial. It could substantially reduce CO_2 emissions and strengthen Libya's energy security by integrating renewable power directly into the national grid.

استرجاع الطاقة الهيدروليكية في شبكات أنابيب المياه: دراسة حالة للنهر الصناعي في ليبيا

أحمد عمر سحاب[*1]، منير محمد الر اقوبي [2]، أسامة امحمد حسين[1]

[1] قسم الهندسة الميكانيكية، مدرسة العلوم الهندسية، الأكاديمية الليبية، طر ابلس، ليبيا

[2]قسم الهندسة الميكانيكية، كلية التقنية الهندسية جنزور، طرابلس، ليبيا

الملخص: يُعَدُّ النهر الصناعي في ليبيا من أكبر مشاريع نقل المياه في العالم، إلا أنه يستهلك كميات ضخمة من الكهرباء لضخ المياه لمسافات طويلة. تسعى هذه الدراسة إلى معالجة تحدي الطلب المتزايد على الطاقة من خلال استرجاع الطاقة الهيدروليكية المهدورة عادةً في صورة فاقد ضغط داخل أنابيب النهر الصناعي. تم إعداد نموذج هيدروليكي للشبكة باستخدام برنامج EPANET اعتماداً على بيانات التصميم الأصلية. جرى تقييم أربع حالات تشغيلية (1.2، 1.3، 2.0، و2.5 مليون متر مكعب يومياً)، وتم تحليل النتائج لتقدير الطاقة القابلة للاسترجاع وتحديد نوع التوربين المناسب. وشملت المنهجية محاكاة توزيع الضغوط والارتفاع الهيدروليكي (head) ، وحسابات الطاقة الممكن استرجاعها، ومقارنتها مع استهلاك المنظومة من الكهرباء. أظهرت النتائج أنه عند معدلات التدفق الحالية (1.2–1.3 مليون م³/يوم) يمكن للتوربينات استرجاع ما بين 686 و733 ميغاواط ساعة يومياً، أي ما يغطي ما يقارب نصف الاستهلاك الكهربائي للنظام. أما عند التدفق التصميمي (2.0 مليون م³/يوم) فينخفض الاسترجاع إلى نحو 610 ميغاواط ساعة يومياً، بينما يتراجع صافي العائد عند 2.5 مليون م³/يوم إلى 117 ميغاواط ساعة يومياً بسبب الحاجة إلى اعادة الضخ للتغلب على انخفاض الضغط الناتج عن زيادة سرعة المياه داخل الانابيب. وتبين أن توربينات فرانسيس هي الأنسب من الناحية العملية، مع إمكانية استخدام توربينات بيلتون في المواقع ذات الضغوط العالية. تؤكد الدراسة أن استرجاع الطاقة من النهر الصناعي ممكن تقنياً وذو جدوى بيئية، حيث يسهم في تقليل انبعاثات ثاني أكسيد الكربون وتعزيز أمن الطاقة في ليبيا عبر ربط هذه الطاقة المتجددة مباشرة بالشبكة الوطنية.

الكلمات المفتاحية:

استرجاع الطاقة، الطاقة الهيدروليكية، النهر الصناعي

1. Introduction

The harvesting of residual hydraulic energy from water transmission and distribution infrastructure has emerged as a vital strategy for improving the sustainability of the water-energy nexus. In conventional pressurized water networks, excess hydraulic head is typically dissipated as waste through pressure-reducing valves (PRVs) or localized friction losses. By replacing or complementing these energy-dissipating components with small-scale hydroelectric turbines, water distribution systems can be transformed from passive energy consumers into localized sources of renewable electricity.

Various turbine technologies are traditionally utilized depending on the specific hydraulic conditions of the host network. Reaction turbines—such as Kaplan, Francis, and Pumps-as-Turbines (PATs)—are generally preferred in low-to-medium head configurations. While Francis designs and PATs offer high efficiency near their operational design points, their performance can degrade sharply under off-design, low-flow conditions [1]. Conversely, impulse turbines, including Pelton and Turgo wheels, maintain high efficiency across highly variable flow regimes [1]. However, impulse configurations are structurally more challenging to implement when downstream residual pressure must be strictly preserved, and they typically demand a higher initial capital expenditure [1]. Recent manufacturing advancements have expanded the viability of these technologies. Compact in-line Francis turbines can now operate within pipe diameters as small as 400 mm to generate up to 1 MW of power [1], while specialized in-pipe impulse arrays, such as Lucid Energy systems, can harvest up to 100 kW per unit at high-pressure nodes without causing catastrophic upstream disruptions.

The viability of such systems has been extensively documented in localized utility networks globally. Power [1] demonstrated micro-hydropower generation ranging from 3 kW to 234 kW across wastewater treatment plants in the UK and Ireland, noting that demographic and climate-driven flow variations dictate turbine selection and long-term efficiency. In agricultural infrastructure, García Morillo [2] used EPANET to model irrigation networks in southern Spain, proving that PATs and conventional Francis turbines could sustainably offset the carbon footprint of intensive agricultural pumping by up to 108 tons of eCO_2. Methodologies for optimizing PAT selection under data-scarce conditions have been further validated by Crespo Chacón [3], demonstrating predictive power modeling accuracies within 0.2%. However, these irrigation and municipal studies feature highly fluctuating, seasonal demand profiles that complicate

continuous generation. More relevant to massive macro-infrastructure is the work of Itani [4] on a large-scale transmission pipeline in western Saudi Arabia. Utilizing WaterCAD and MATLAB simulations, that study identified localized high-pressure hotspots suitable for Pelton turbines, projecting a total installed capacity of 5,751 kW and a reduction of 35,295 tons of annual eCO_2. This underscored that high-pressure, continuous-flow transmission pipelines offer significantly higher stability and commercial viability than fluctuating distribution networks.

Despite these global insights, a significant research gap persists regarding the integration of energy recovery systems within unique, ultra-large-scale water conveyance infrastructures operating under severe regional energy constraints. Libya presents a critical case study for this dynamic. The country has faced a chronic deficit in electrical generation capacity for several years, resulting in severe rolling blackouts and a continuous strain on the national grid. Simultaneously, Libya relies fundamentally on the Man-Made River (MMR) Project—one of the largest closed, pressurized water transport systems in the world—to deliver massive quantities of water over thousands of kilometers. Operating the MMR requires vast amounts of electrical energy, primarily consumed by massive wellfield and station pumps. While the system is heavily optimized for volume delivery, the enormous amounts of hydraulic energy dissipated as pressure drops within its extensive pipeline network represent an unmapped resource for self-sustained clean energy generation.

This research addresses these parallel challenges by evaluating the technical feasibility and environmental benefits of hydropower recovery within the Jabel Al-Hasawna–Al-Jfara pipeline, a primary artery of the MMR system. By constructing a comprehensive hydraulic model of the pipeline utilizing EPANET and actual industrial design data, this study analyzes the complex head and pressure distributions under multiple operational flow scenarios. The primary objectives are to:

- Identify optimal spatial locations for turbine integration based on elevation profiles and pressure margins.
- Quantify the net daily electrical energy output retrievable across varying operational scenarios.
- Determine the most robust turbine technology and configuration (series versus parallel) capable of handling the pipeline's high-head, high-volume environment.
- Assess downstream pressure impacts to ensure that energy harvesting does not compromise the core water supply mandate of the infrastructure.

By integrating these findings, this study provides a scalable framework for converting critical water transmission corridors into reliable contributors to national energy security.

2. Materials and Methods

2.1 Study Area and System Description

This study investigates hydropower energy recovery potential within the Western Libya System (WLS), a critical segment of the Man-Made River Project (MMRP) Phase II. The WLS conveys groundwater from the East Jabal Hasouna (EJH) and North East Jabal Hasouna (NEJH) wellfields to coastal demand centers including Tripoli, Garabulli, and the Jeffara Plain. Water is initially pumped 47 km to the Fezzan Regulating Station (545 m AMSL), then flows by gravity through the Ash Shwayrif Flow Control Station (319.5 m AMSL), where the pipeline bifurcates into the Central Branch (0.834 MCMD design flow to Tarhunah) and Eastern Branch (1.166 MCMD to Tripoli) [8]. The total elevation drop of approximately 490 m between Fezzan and coastal terminals (~54 m AMSL) establishes a substantial hydraulic gradient suitable for energy recovery.

2.2 Pipeline Specifications and Data Collection

The pipeline network comprises approximately 983 km of Prestressed Concrete Cylinder Pipe (PCCP) conforming to AWWA C301-84 structural standards [8]. Internal diameters range from 2400 to 4000 mm across major conveyance segments. Internal surfaces are lined with Thanecoat polyurethane coating to reduce corrosion and friction; an absolute roughness height (ε) of 0.000265 m (0.265 mm) was adopted to represent mid-life pipe conditions in hydraulic calculations. Design and operational data—including pipe lengths, diameters, elevations, flow rates, and pressure ratings—were obtained from official MMRP technical documentation and hydraulic grade line sheets [8].

Table (1). Pipe diameters and design flow capacities along the Western Libya System pipeline.

Segment	Diameter (mm)	Design Flow (MCMD)
EJH to Fezzan Regulating Station	4000	1.389
Fezzan to NEJH(S) Junction	4000	1.658
NEJH(N) Junction to Ash Shwayrif FCS	3600–4000	2.000
Ash Shwayrif FCS to Tarhunah Regulating Station	3600–4000	0.834
Ash Shwayrif FCS to Garabulli	3600–4000	1.166 (1.666 max)

Table (2). Elevation data for key locations in the Western Libya System.

Location	Elevation (m AMSL)
Fezzan Regulating Station	545.0
Ash Shwayrif Flow Control Station	319.5
Garabulli Terminal	54.5
Bin Ghashir Terminal	54.0

2.3 Hydraulic Modeling and Simulation

Hydraulic simulations were performed using EPANET version 2.2, a public-domain software developed by the U.S. Environmental Protection Agency (Washington, D.C., USA) for modeling pressurized pipe networks [7]. The network was constructed with nodes representing junctions, tanks, and control stations, and links representing pipes with assigned lengths, diameters, roughness coefficients, and elevation profiles. All simulations were executed in steady-state mode using the implicit Gradient Method solver with a convergence tolerance of 0.001.

Head loss due to friction was calculated using the Darcy–Weisbach equation:

$$h_f = f \cdot \frac{L}{D} \cdot \frac{v^2}{2g} \cdot \qquad 1$$

where *hf* is friction head loss (m), *f* is the Darcy friction factor, L is pipe length (m), D is internal diameter (m), v is mean flow velocity (m/s), and *g* is gravitational acceleration (9.81 m/s²). The friction factor f was solved iteratively using the Colebrook–White equation for turbulent flow:

$$\frac{1}{\sqrt{f}} = -2log_{10}\left(\frac{\varepsilon}{3.7D} + \frac{2.51}{Re.\sqrt{f}}\right) \quad \ldots\ldots 2$$

where Re is the Reynolds number, computed as

$$Re = \rho v D/\mu. \quad \ldots\ldots 3$$

Water was modeled as an incompressible fluid at 20°C with density ρ = 1000 kg/m^3 and dynamic viscosity μ = 1.002 × 10^{-3} Pa·s. Minor losses from fittings, bends, and control structures were computed using with empirical loss coefficients K assigned based on fitting type.

$$h_m = K.\frac{v^2}{2g} \quad \text{..... 4}$$

2.4 Operational Flow Scenarios and Design Constraints

Four representative flow scenarios were simulated based on historical operation and design specifications: 1.2 and 1.3 MCMD (current sustained output), 2.0 MCMD (original Phase I design capacity), and 2.5 MCMD (planned Phase II expansion). Scenario 2 (1.3 MCMD) was selected as the primary modeling basis, representing steady-state long-term operation while avoiding surge-related transients.

Table (3). Operational flow scenarios simulated in the hydraulic model.

Scenario	Total Flow (MCMD)	Eastern Route (MCMD)	Central Route (MCMD)	Classification
1	1.20	0.70	0.50	Operational output (1996)
2	1.30	0.76	0.54	Improved output (2006)
3	2.00	1.166	0.834	Phase 1 design capacity
4	2.50	1.666	0.834	Phase 2 expansion

To ensure structural integrity and operational safety, the following constraints were enforced during simulation and post-processing:

- Minimum residual pressure head ≥ 2.0 m above pipe crown at all locations to prevent air entrainment and column separation
- Maximum flow velocity ≤ 2.0 m/s to limit erosion and control water hammer effects
- Surge pressure allowance ≤ 140% of nominal rating for pipes rated 6–10 bar, or +4 bar for pipes >12 bar

2.5 Turbine Simulation and Energy Recovery Calculations

Hydro turbines were simulated within EPANET by replacing pressure-reducing valves with General Purpose Valve (GPV) elements configured to enforce target head drops (ΔH) while maintaining downstream residual pressure above the 2.0 m safety threshold. This approach accurately represents the pressure dissipation behavior of in-line turbines while verifying that water delivery performance remains uncompromised.

Post-processing and energy calculations were performed using Microsoft Excel version 2021 (Microsoft Corporation, Redmond, Washington, USA). Recoverable hydraulic power (P) and annual energy yield (E) were computed using:

$$P = \rho.g.Q.H.\eta \quad \text{..... 5}$$

$$E = \frac{P.t}{1000} \quad \text{..... 6}$$

where Q is flow rate (m^3/s), H is net available head (m), η is combined turbine-generator efficiency (typically 0.75–0.9 based on manufacturer performance data for Francis turbines), and t is operational time (8760 h/year for continuous operation). The division by 1000 converts results from watt-hours to kilowatt-hours.

2.6 Turbine Selection and Placement Criteria

Turbine type selection was based on matching simulated head and flow conditions at candidate sites to established operational envelopes for conventional hydro turbines [5,6]. Francis turbines (medium-head, high-flow) were prioritized for most locations due to their compact inline designs and high efficiency (85–94%) across variable operating conditions. Pelton turbines (high-head, low-flow) were considered as alternatives for high-head segments (>150 m). Kaplan turbines were excluded due to the system's predominantly medium-to-high head profile.

Table (4). Turbine types considered for energy recovery applications.

Turbine Type	Head Range (m)	Flow Range (m^3/s)	Efficiency (%)	Typical Application
Pelton	150–1500	0.01–5	80–92	High-head, low-flow pipelines
Francis	10–300	0.1–100	85–94	Medium-head, high-flow systems
Kaplan	2–40	1–200	80–90	Low-head, high-flow conveyance
PAT	10–100	0.05–10	60–80	Irrigation, low-pressure zones

Candidate installation sites were ranked using three primary criteria:

- **Energy density**: Nodes maximizing the product Q·H were prioritized to maximize return on investment
- **Infrastructural accessibility**: Preference was given to existing flow control stations (e.g., Ash Shwayrif, Wadi Al-Tumalah) to leverage bypass infrastructure, telemetry systems, grid connections, and maintenance access, minimizing civil works and project execution time

2.7 Environmental Impact Assessment

Carbon emission reductions were estimated using a grid emission factor of 0.6 kg CO_2/kWh, representative of Libya's fossil-fuel-dominated electricity generation mix [4]. Avoided emissions (CO_2) were calculated as:

$$\mathbf{CO_2 avoided = E recovered \times EF grid}$$

where E is annual recovered energy (kWh) and EFgrid is the emission factor. This simplified approach provides a conservative estimate of environmental benefit without requiring detailed lifecycle assessment.

2.8 Model Validation

Simulation results were validated against original MMRP hydraulic grade line data at the Ash Shwayrif Flow Control Station, the system's critical bifurcation point. Simulated head values were compared to design values across multiple flow rates; deviations ranged from 0.8% at low flows to 6.3% at high flows, all within acceptable engineering limits for steady-state modeling of aged infrastructure. This validation confirms the reliability of the adopted modeling approach for subsequent energy recovery analysis.

This section should provide sufficient detail to enable the study to be reproduced by other researchers. Previously published methods should be properly cited, and any modifications to established procedures must be clearly described. The names, models, manufacturers, and locations (city and country) of equipment, instruments, software, and reagents should be specified where relevant. Authors are encouraged to organize this section using appropriate subheadings for clarity and readability.

3. Results

Hydraulic simulations of the Man-Made River pipeline were conducted in EPANET under steady-state conditions to evaluate pressure distribution and hydroelectric energy recovery potential at existing flow

control stations. Four operational scenarios were modelled at flow rates of 1.2, 1.3, 2.0, and 2.5 million cubic meters per day (MCMD), representing current production levels through to maximum design capacity. Figure 1illustrates the topographic profile and hydraulic layout of the transmission network utilized for EPANET modeling. The pipeline is segmented at the primary junction point into the shared Main Line (blue), the continuing coastal Eastern Branch (green), and the diverging inland Central Branch (orange, dashed). Key municipal demand nodes and delivery stations are annotated along the profile to map geographic locations directly to their respective hydraulic elevations.

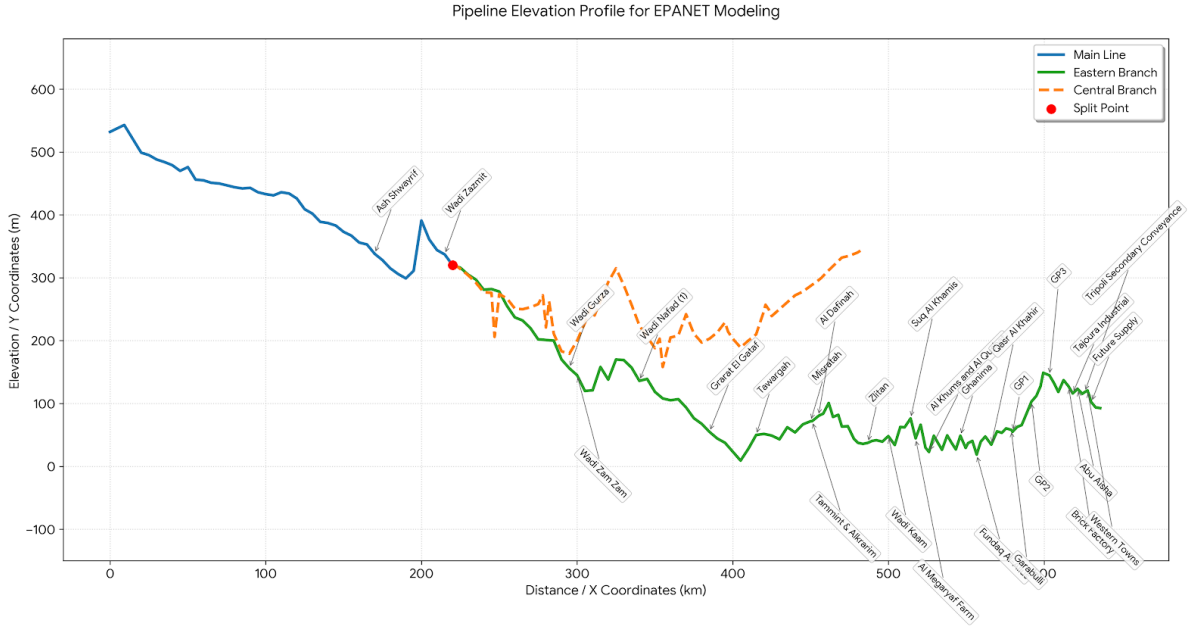

Figure (1). Elevation profile of the pipeline network showing the Main Line, Eastern Branch, and Central Branch configurations for EPANET modeling.

3.1 Hydraulic Performance and Pressure Profiles

Simulations assumed gravity-driven flow with zero gauge pressure at the inlet, constant pipe roughness (0.267 mm), and minor losses calculated as K = 0.049 × (L/1000). Pressure and hydraulic head profiles were generated for each scenario without pressure control valves to identify zones of excess pressure suitable for turbine installation.

Figure (2) presents the simulated pressure distribution for all scenarios, color-coded by pipeline section. The pipeline begins as a single main line (Southern section) and splits at 210.882 km into the Central and Eastern branches. Maximum pressure points are highlighted, revealing where pressure accumulates along the route. These high-pressure zones are critical for identifying optimal locations for energy recovery turbines.

Figure (3) presents the head profiles along the pipeline for multiple simulated flow scenarios. The vertical dashed red line at 210.882 km denotes the pipeline split point. Each colored curve corresponds to a specific flow rate under conditions without pressure control valves, except for the 2.5 MCMD case where a pump is required to maintain delivery pressure in the Central branch. The results illustrate the progressive decrease in hydraulic head due to frictional losses, with higher flow rates exhibiting steeper head declines. Downstream of the split, head gradients differ between branches, reflecting their distinct hydraulic characteristics.

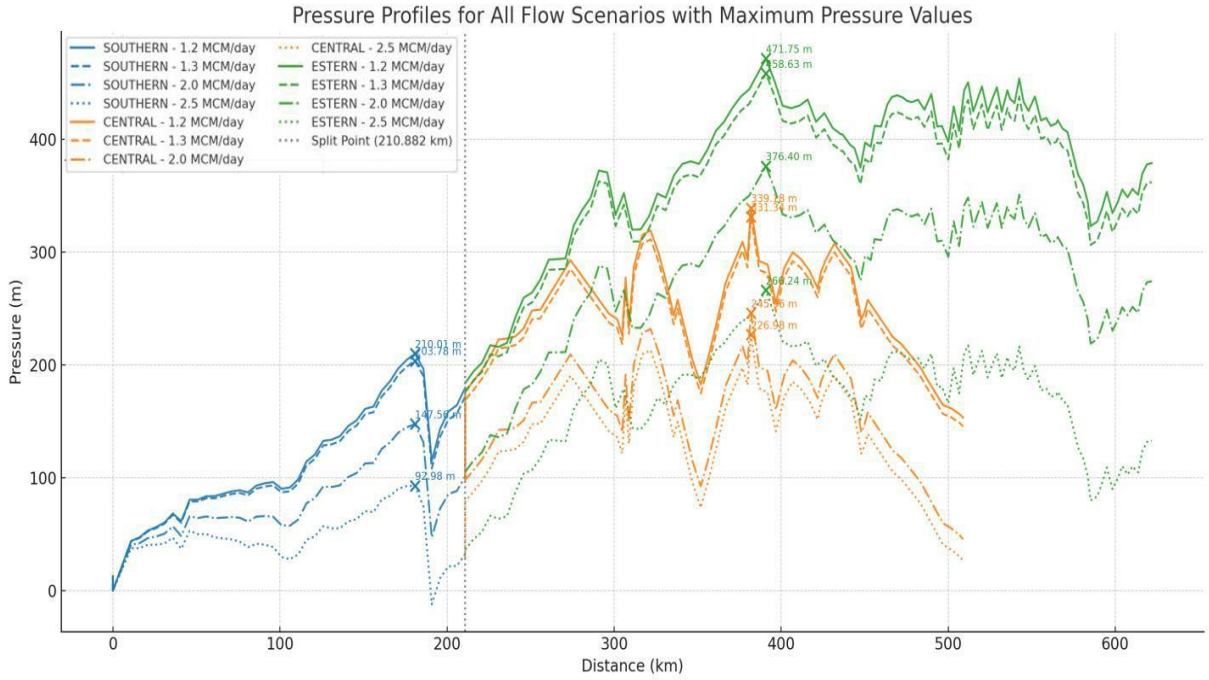

Figure (3). Pressure profiles for all flow scenarios (1.2–2.5 MCMD) by pipeline section, with maximum pressure points labelled and the split location at 210.882 km.

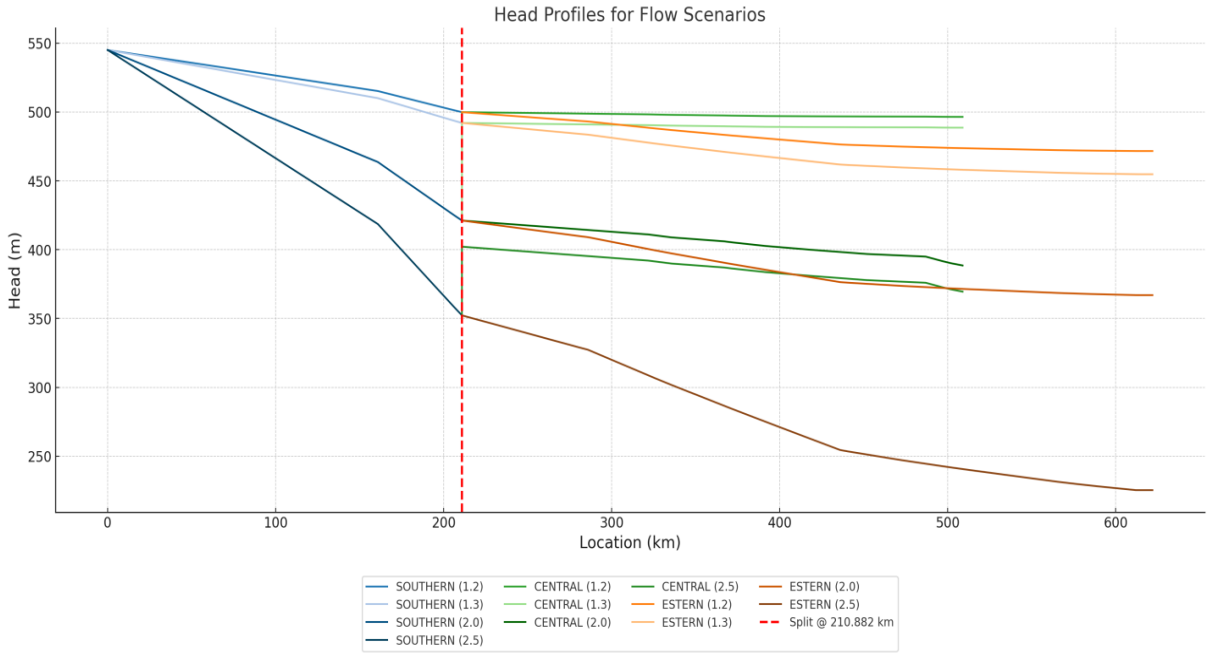

Figure (4). Head profiles along the pipeline for different flow scenarios without valves, except for the 2.5 MCMD case where a pump is required to maintain the required pressure in the Central branch.

3.2 Scenarios Comparison

Scenario 1 – Baseline at 1.2 MCMD

Figure (4) presents the head and pressure profiles for the 1.2 MCMD scenario with hydro turbines installed. The profile is segmented into Southern, Central, and Eastern sections, with the split point at 210.882 km. The maximum head of 545.00 m occurs near the inlet, while the maximum pressure of 223.60 m is observed downstream in the Eastern section. At the split point, head and pressure are 351.01 m and 31.01 m, respectively. Pressure reduction patterns correspond to turbine placement locations, confirming that turbine positioning in high-pressure segments effectively lowers excess pressure while providing substantial energy harvesting potential.

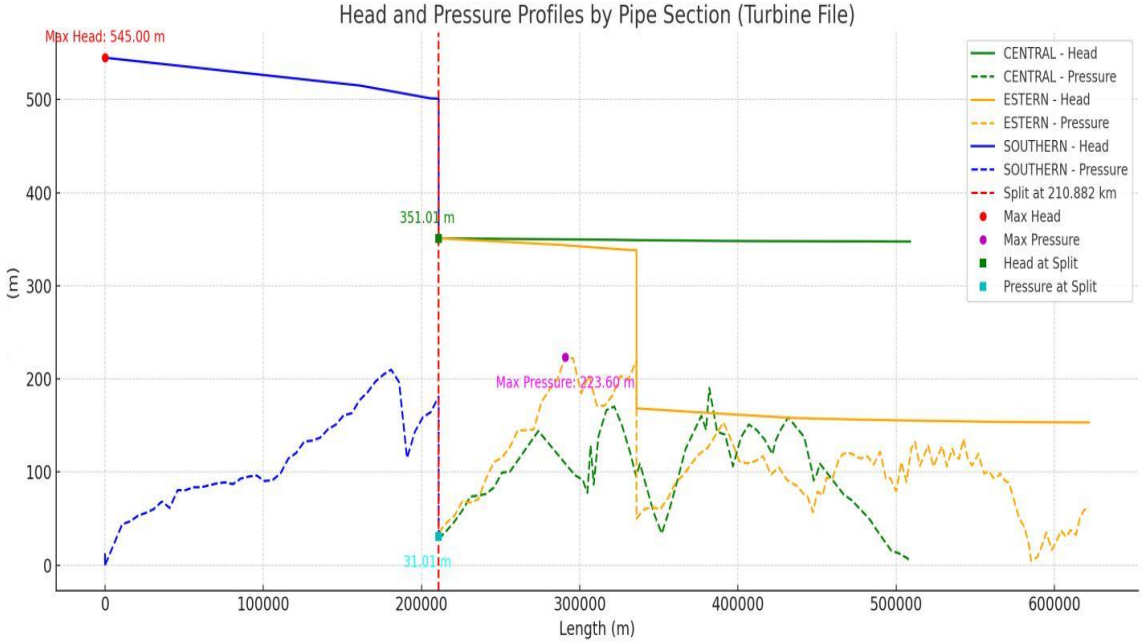

Figure (5) .Head and pressure profiles along the pipeline for the 1.2 MCMD scenario with hydro turbines installed.

Table (5) summarizes the hydraulic parameters obtained from EPANET simulation at 1.2 MCMD with turbines installed. Table (6) presents the embedded and recoverable hydropower potential at 85% turbine efficiency.

Table (5). Hydraulic parameters from EPANET simulation at 1.2 MCMD.

Link ID	Diameter (mm)	Flow (m^3/s)	Velocity (m/s)	Unit Headloss (m)
ASH	4000	13.37	1.06	150.00
SHWAYRIF_TURBINE				
TUMALAH_TURBINE	3600	8.40	0.83	170.01

Table (6) . Recoverable hydropower potential for Scenario 1 (1.2 MCMD, η = 85%).

Turbine	Flow (m^3/s)	Head (m)	Recoverable Power (MW)	Energy/day (MWh)
Ash Shwayrif	13.37	150	16.69	400.66
Wadi Al-Tumalah	8.40	170	11.90	285.60
Total	—	—	28.59	686.26

Scenario 2 – Baseline at 1.3 MCMD

At 1.3 MCMD, increased flow velocities result in greater frictional head losses. Table (7). Summarizes the hydraulic parameters, and Table(8).presents the recoverable energy potential.

Table (7). Hydraulic parameters from EPANET simulation at 1.3 MCMD.

Link ID	Diameter (mm)	Flow (m^3/s)	Velocity (m/s)	Headloss (m)
ASH SHWAYRIF_TURBINE	4000	14.55	1.43	145.00
WADI AL-TUMALAH_TURBINE	3600	9.58	0.94	162.48

Table (8). Recoverable hydropower potential for Scenario 2 (1.3 MCMD, η = 85%).

Turbine	Flow (m^3/s)	Head (m)	Recoverable Power (MW)	Energy/day (MWh)
Ash Shwayrif	14.55	145	17.59	422.08
Wadi Al-Tumalah	9.58	162.48	12.96	311.10
Total	—	—	30.55	733.18

Scenario 3 – Baseline at 2.0 MCMD

At the initial design capacity of 2.0 MCMD, higher flow velocity results in lower pressure levels compared to lower-flow scenarios, with pressures closer to pipeline design limits. Table (9) summarizes hydraulic parameters, and Table (10) presents the recoverable energy.

Table (9). Hydraulic parameters from EPANET simulation at 2.0 MCMD.

Link ID	Diameter (mm)	Flow (m^3/s)	Velocity (m/s)	Headloss (m)
ASH SHWAYRIF_TURBINE	4000	22.63	1.80	43.99
TUMALAH_TURBINE	3600	11.73	1.15	175.00

Table (10). Recoverable energy for Scenario 3 (2.0 MCMD, η = 85%).

Turbine Location	Flow (m^3/s)	Head (m)	Recoverable Power (MW)	Energy/day (MWh)
Ash Shwayrif	22.63	43.99	8.29	199.0
Wadi Al-Tumalah	11.73	175.00	17.12	410.9
Total	34.36	—	25.41	609.9

Scenario 4 – Baseline at 2.5 MCMD

At 2.5 MCMD, increased velocity produced greater head losses, reducing residual pressure at the split point to only 32 m. A pumping station at Ash Shwayrif was required to sustain flow through the Central branch. Figure (5) and Figure (6) present the head and pressure profiles without and with turbines, respectively. Table (11) summarizes the hydraulic status of active links, and Table (12) presents the net energy balance.

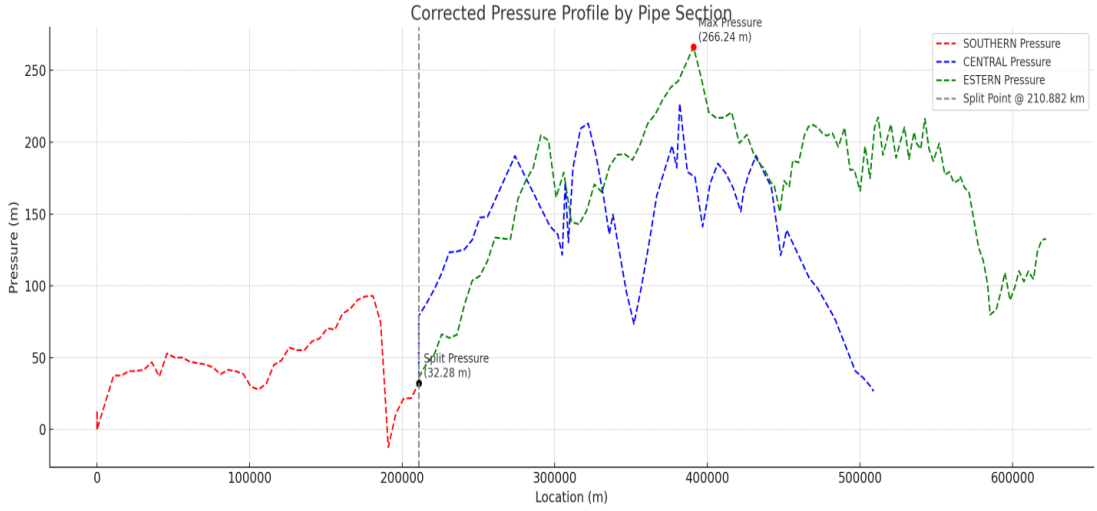

Figure (6). EPANET-simulated head and pressure profiles at 2.5 MCMD without valves.

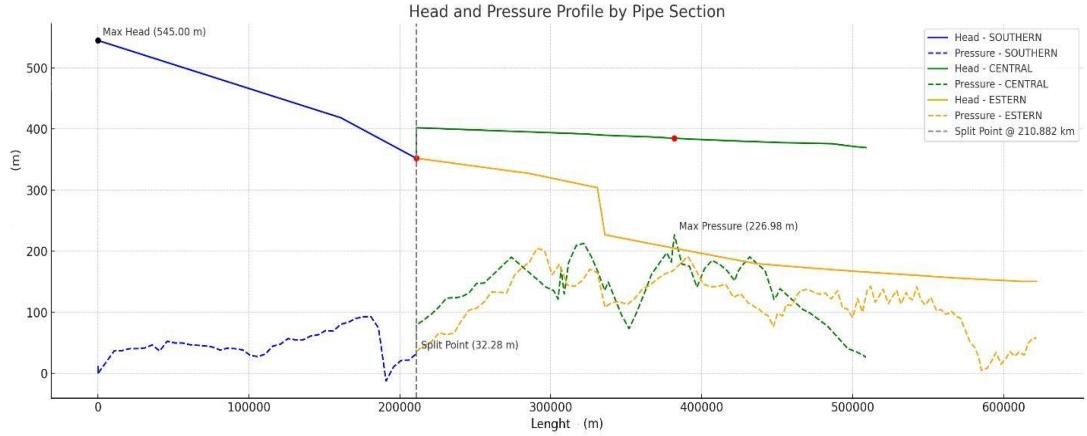

Figure(7).Head and pressure profiles along the pipeline for the 2.5 MCMD scenario with hydro turbines installed

Table (11). Hydraulic parameters from EPANET simulation at 2.5 MCMD.

Link ID	Diameter (mm)	Flow (m^3/s)	Velocity (m/s)	Unit Headloss (m)	Status
PUMP_ASH SHWAYRIF	—	9.65	0	-50.00	Open
WADI TUMALAH_TURBINE	3600	17.52	1.72	76.59	Open
ASH SHWAYRIF_TURBINE	3600	0	0	0	Closed

Table (12). Net power and daily energy evaluation for Scenario 4 (2.5 MCMD).

Device	Flow (m^3/s)	Head (m)	Efficiency (%)	Power at η (MW)	Energy/day at η (MWh)
Pump – Ash Shwayrif	9.65	50.00	75	6.32 (input)	151.7 (input)
Turbine – Wadi Tumalah	17.52	76.59	85	11.20 (output)	268.8 (output)
Net (Turbine – Pump)	—	—	—	+4.88	+117.1

3.3 Model Validation

Table (13) compares simulated hydraulic grade line (HGL) values at Ash Shwayrif Flow Control Station with original design data. Differences ranged from 0.8% at zero flow to 6.3% at 2.0 MCMD, confirming model reliability within acceptable engineering tolerances.

Table (13). Comparison of Hydraulic Grade Line (HGL) values at Ash Shwayrif.

Flow Rate (MCMD)	Designer HGL (m)	Simulated HGL (m)	Difference (m)	% Difference
0	549.4	545.0	-4.4	0.80%
0.834	529.79	520.51	-9.28	1.75%
1.16	514.22	502.36	-11.86	2.31%
1.66	479.99	458.72	-21.27	4.43%
2.0	449.5	421.15	-28.35	6.31%

3.4 Turbine Selection

Figure (7) illustrates the operational ranges of conventional hydro turbine types in terms of head and flow rate. Table (14) summarizes the turbine selection results for all scenarios based on simulated hydraulic conditions. Francis turbines were identified as the most suitable technology for both sites across all scenarios, operating efficiently within medium-to-high head (44–175 m) and high-flow (8.4–22.6 m^3/s) ranges. Pelton turbines represent a feasible alternative at Wadi Al-Tumalah where head exceeds 160 m.

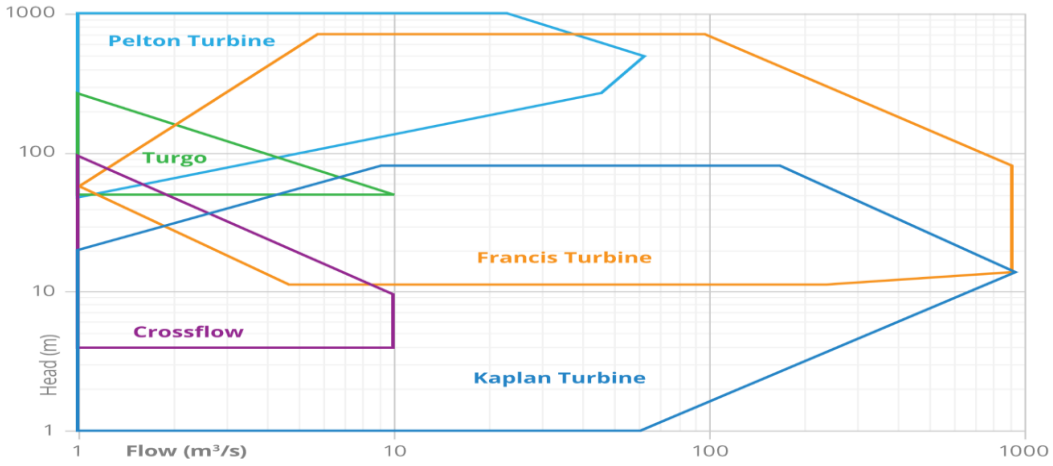

Figure (8). Turbine selection graph.

Table (14). Turbine selection results for all scenarios.

Scenario	Location	Flow (m^3/s)	Head (m)	Suitable Turbine Type	Notes
S1 (1.2 MCMD)	Ash Shwayrif	13.37	150	Francis	Medium–high head, large flow
S1 (1.2 MCMD)	Wadi Al-Tumalah	8.40	170	Francis / Pelton	Overlap region; Francis preferred
S2 (1.3 MCMD)	Ash Shwayrif	14.55	145	Francis	Optimal for medium–high head
S2 (1.3 MCMD)	Wadi Al-Tumalah	9.58	162.5	Francis / Pelton	Both feasible
S3 (2.0 MCMD)	Ash Shwayrif	22.63	44	Francis	Low–medium head, high flow
S3 (2.0 MCMD)	Wadi Al-Tumalah	11.73	175	Francis / Pelton	High head, moderate flow
S4 (2.5 MCMD)	Ash Shwayrif	0	0	—	Turbine off in this scenario
S4 (2.5 MCMD)	Wadi Al-Tumalah	17.52	76.6	Francis	Medium head, high flow

3.5 Energy Recovery versus Electricity Consumption

Annual electricity consumption was estimated from historical production data (2021–2024) using specific energy consumption values (1.23–1.352 kWh/m^3). Table (15)presents the derived water production rates.

Table (15). Water production derived from electricity consumption (2021–2024).

Year	SEC (kWh/m^3)	Total Electricity (MWh/yr)	Annual Volume (m^3)	Daily (MCM/d)	Flow (m^3/s)
2024	1.23	486,005	3.95×10^8	1.083	12.5
2023	1.352	501,371	3.71×10^8	1.016	11.8
2022	1.352	503,172	3.72×10^8	1.020	11.8
2021	1.30	395,634	3.04×10^8	0.834	9.7

Table (16) summarizes the recovered energy at 85% turbine efficiency for all scenarios. Table (17) compares annual recovered energy with scaled electricity consumption estimates.

Table (16). Recovered energy at 85% efficiency for selected scenarios.

Scenario (MCMD)	Location	Flow (m^3/s)	Head (m)	Recovered Power (MW)	Energy/day (MWh)
1.2	Ash Shwayrif	13.37	150	16.69	400.7
	Wadi Al-Tumalah	8.40	170	11.90	285.6
	Total			28.59	686.3
1.3	Ash Shwayrif	14.55	145	17.59	422.1
	Wadi Al-Tumalah	9.58	162.5	12.96	311.1
	Total			30.55	733.2
2.0	Ash Shwayrif	22.63	44	8.29	199.0
	Wadi Al-Tumalah	11.73	175	17.12	410.9
	Total			25.41	609.9
2.5	Net (after pump)	17.52	76.6	4.88	117.1

Table (17). Comparison of recovered hydropower with electricity consumption.

Scenario (MCMD)	Annual Recovery (MWh/yr)	Consumption (MWh/yr)	Coverage (%)
1.2	250,485	538,740	46.5
1.3	267,611	583,635	45.9
2.0	222,614	897,900	24.8
2.5	42,742	1,122,375	3.8

Recovery potential peaked at 1.3 MCMD, covering approximately 46% of estimated consumption. Coverage declined at higher flows due to increased frictional losses and pumping requirements.

3.6 Carbon Emission Reduction

Using a grid emission factor of 0.6 tCO_2/MWh, avoided CO_2 emissions ranged from 25,645 t/yr at 2.5 MCMD to 160,567 t/yr at 1.3 MCMD (Table (18)).

Table (18). Estimated annual CO_2 emission reductions from recovered hydropower.

Scenario (MCMD)	Annual Recovery (MWh/yr)	Avoided CO_2 (t/yr)
1.2	250,485	150,291
1.3	267,611	160,567
2.0	222,614	133,568
2.5	42,742	25,645

4. Discussion

4.1 Hydraulic Dynamics and Flow-Dependency of Energy Recovery

EPANET simulations reveal a non-linear relationship between pipeline flow rates and net energy recovery. As volumetric throughput scales from 1.2 MCMD to 2.5 MCMD, fluid velocities within the 3600–4000 mm lines rise from 1.06 m/s to 1.80 m/s, causing friction-induced head losses to escalate exponentially. Consequently, the excess hydraulic head available at Ash Shwayrif collapses from 150 m to 44 m at 2.0 MCMD. At 2.5 MCMD, natural gravity head is so severely depleted that a 50 m booster pump is required to sustain flow in the Central Branch, parasitically consuming 6.32 MW of the 11.20 MW generated downstream. Thus, energy recovery peaks sharply under current outputs (1.2–1.3 MCMD), where high volumetric mass flow and localized pressure heads reach an optimal equilibrium.

4.2 Comparative Analysis with Existing Literature

The continuous gravity-flow profile of the Western Libya System provides superior generation stability compared to localized municipal or agricultural distribution networks found in the literature. The networks reviewed by Power [1] and García Morillo [2] were limited by severe demographic or seasonal flow fluctuations, complicating grid integration and making low-efficiency Pumps-as-Turbines (PATs) [3] structurally unsuited for this scale. Compared to Itani's [4] transmission pipeline study in Saudi Arabia, which projected a 5.75 MW capacity, the Jabel Al-Hasawna–Al-Jfara pipeline yields a vastly superior profile. At 1.3 MCMD, its combined output reaches an installed capacity of 30.55 MW (733.18 MWh/day), offsetting up to 160,567 tons of CO_2 annually due to its massive volumetric flow rates over a sustained 490 m drop.

4.3 Practical Relevance and Technical Limitations

Integrating inline Francis turbines directly into existing flow control stations provides a decentralized solution to Libya's chronic electrical deficits, allowing the water infrastructure to internally offset approximately 46% of its own pumping consumption. Utilizing existing facilities minimizes civil works and grid interconnection timelines. However, full-scale implementation is bound by strict operational safeguards:

Pressure Constraints: Turbines must maintain a minimum residual pressure head of 2.0 meter above the pipe crown to prevent catastrophic column separation and line collapse.

Transient Risks: Sudden electrical grid trips can cause turbine runaway, necessitating fast-acting synchronous bypass valves and surge tanks to absorb water hammer transients within the 140% nominal pressure safety allowance.

Pipe Aging: The 0.8–6.3% model validation discrepancy underscores system sensitivity to interior pipe roughness (ε = 0.265mm); long-term yields could gradually decline unless rigorous pipeline maintenance and pigging schedules are enforced.

5. Conclusions

This study evaluated the hydraulic performance and hydroelectric energy recovery potential of Libya's Man-Made River (MMR) pipeline using steady-state EPANET simulations across four operational scenarios (1.2–2.5 MCMD). The principal findings demonstrate that integrating hydro turbines at existing flow control stations offers a technically viable and strategically valuable pathway to offset the system's substantial operational electricity demand.

Simulations revealed that the highest energy recovery potential occurs at current operating flows (1.2–1.3 MCMD), yielding up to 733 MWh/day and covering approximately 46% of the system's estimated annual electricity consumption. Recovery efficiency is strongly flow-dependent: increasing discharge to the initial design capacity (2.0 MCMD) reduces coverage to 25%, while operating at 2.5 MCMD requires pumping assistance at Ash Shwayrif, drastically lowering net recovery to 117 MWh/day (~4% coverage). Model validation against original design data showed hydraulic grade line discrepancies of only 0.8–6.3%, confirming the reliability of the simulation framework within accepted engineering tolerances. Francis turbines were identified as the most suitable technology across all viable scenarios, with Pelton units serving as a feasible alternative at high-head locations. Environmentally, the proposed configuration could avoid 25,600–160,600 tCO_2 annually, significantly outperforming comparable pipeline recovery projects in the region.

These outcomes underscore the practical value of repurposing existing pressure control infrastructure for decentralized renewable energy generation. By leveraging established bypass lines, control systems, and the pipeline's alignment with high-voltage transmission corridors, turbine integration can be achieved with minimal civil works and streamlined grid interconnection. This approach directly enhances operational sustainability, reduces reliance on fossil-fuel-based generation, and supports Libya's broader climate and energy security objectives.

To advance implementation, pilot-scale installations at Ash Shwayrif and Wadi Al-Tumalah are recommended, prioritizing operation at 1.2–1.3 MCMD where hydraulic conditions and recovery efficiency are optimal. Future research should incorporate transient hydraulic analysis to evaluate surge propagation and water hammer risks, alongside comprehensive techno-economic assessments (CAPEX, OPEX, and payback periods). Investigating modular inline turbine technologies, hybrid renewable microgrids at control stations, and the planned parallel pipeline for high-flow operations will further enhance system resilience and scalability. Establishing long-term instrumentation and adaptive control protocols will also be essential to validate simulation predictions and optimize real-world performance.

Ultimately, this research provides a validated, reproducible framework for transforming large-scale water conveyance networks into dual-purpose infrastructure, delivering both reliable water supply and clean energy while offering a scalable model for sustainable pipeline management in water-scarce regions worldwide.

6. References

[1]. C. Power, A. McNabola, and P. Coughlan, "Development of an evaluation method for hydropower energy recovery in wastewater treatment plants: Case studies in Ireland and the UK," Sustainable Energy Technologies and Assessments, vol. 7, pp. 166–177, Sep. 2014, doi: 10.1016/j.seta.2014.06.001.

[2]. J. García Morillo, A. McNabola, E. Camacho, P. Montesinos, and J. A. Rodríguez Díaz, "Hydro-power energy recovery in pressurized irrigation networks: A case study of an Irrigation District in the South of Spain," Agricultural Water Management, vol. 204, pp. 17–27, May 2018, doi: 10.1016/j.agwat.2018.03.035.

[3]. M. Crespo Chacón, J. A. Rodríguez Díaz, J. García Morillo, and A. McNabola, "Hydropower energy recovery in irrigation networks: Validation of a methodology for flow prediction and pump as turbine selection," Renewable Energy, vol. 147, pp. 1728–1738, Mar. 2020, doi: 10.1016/j.renene.2019.09.119.

[4]. Y. Itani, M. R. Soliman, and M. Kahil, "Recovering energy by hydro-turbines application in water transmission pipelines: A case study west of Saudi Arabia," Energy, vol. 211, p. 118613, Nov. 2020, doi: 10.1016/j.energy.2020.118613.

[5]. M. Chaudhry, Applied Hydraulic Transients, 3rd ed., Springer, 2014.

[6]. A. Harvey, A. Brown, P. Hettiarachi, and A. Inversin, Micro-Hydro Design Manual: A Guide to Small-Scale Water Power Schemes, 2nd ed., ITDG Publishing, 2020.

[7]. L. A. Rossman, EPANET 2: Users Manual, U.S. Environmental Protection Agency, Cincinnati, OH, USA, 2000. [Online]. Available: https://www.epa.gov/water-research/epanet

[8]. Great Man-Made River Authority (GMRA), Final Hydraulic Report: Phase I and II, Tripoli, Libya, 2006.